

Radiation Physics and Engineering 2024; ?(?):?–?

# Exploring the applications of low energy ion accelerators through exothermic nuclear reaction products

Zeinab Sadat Imani<sup>a</sup>, Omidreza Kakuee<sup>b,\*</sup>, Yavar Taghipour Azar<sup>b</sup>, Amir Abbas Sabouri Dodaran<sup>a</sup>

<sup>a</sup>Department of Physics, Payam Noor University, P.O. Box 19395-3697, Tehran, Iran

<sup>b</sup>Physics & Accelerators Research School, Nuclear Science and Technology Research Institute, P.O. Box, 14395-836, Tehran, Iran

## HIGHLIGHTS

- Nuclear reactions were used to produce light, energetic, and low-flux ions as a secondary beam.
- The laboratory setup facilitated secondary reaction products and their interaction with the sample.
- The exothermic nuclear reactions yielded approximately  $10^6$  secondary  $H^+$  and  $He^+$  particles.
- These particles are with energies in the range of 4 to 18.5 MeV.

## ABSTRACT

The production of light, energetic and low-flux ions as a secondary beam caused by nuclear reaction can be used in various branches of nuclear physics. Due to the limited availability of energy in small laboratories equipped with electrostatic accelerators, accessing energetic light particles is crucial. For this purpose, selected nuclear reactions were introduced. In this research, primary proton, deuterium and helium-3 beams with energy less than 2 MeV were used for samples with a thickness of  $10^{19}$  atom.cm<sup>-2</sup> and the yield of reactions was obtained. The laboratory setup was designed in such a way that in addition to the access to the nuclear reaction products with a suitable yield, favorable conditions were provided for the extraction and transfer of the reaction products as well as their interaction with the sample. In these exothermic nuclear reactions, the yield is in the order of  $10^6$  particles and secondary proton and alpha particles with energies of 4 to 18.5 MeV have been obtained. Also, the selected reactions are in accordance with the radiation protection protocols of similar laboratories.

## KEYWORDS

Ion beam application  
Nuclear reaction  
Reaction yield  
Secondary ion beam

## HISTORY

Received: 24 January 2024  
Revised: 6 March 2024  
Accepted: 13 March 2024  
Published: In Press

## 1 Introduction

Electrostatic accelerators, are cost-effective and find wide application in both fundamental and applied physics. These ion accelerator systems, designed to generate stable MeV ion beams with a few  $\mu A$  current and energy resolution in the range of a few hundred electron volts, serve various purposes. They are crucial for nuclear methods, enabling research on material properties, environmental monitoring, biomedical investigations, and the study of cultural heritage artifacts, among other uses. Moreover, these accelerators are used for irradiation, deep implantation, lithography (Durante et al., 2019; Bhandari and Dey, 2011).

By the way, for irradiating semiconductor materials, biological samples, semiconductor chips, and ion imaging,

low-intensity proton and alpha ion beams are employed (Granja et al., 2022). The production of these beams holds significant importance. A facility that provides ion beams with a sufficient range to irradiate the mentioned samples is crucial. In these applications, single ion or ions with a fractional intensity of fA are irradiated to the sample. For a qubit, this radiation modifies the electronic structure of the semiconductor (Jamieson et al., 2002; McCallum et al., 2012). Also, this ion radiation can be used to study semiconductor samples. The collision of the ion beam with the semiconductor or insulator sample causes a current to be induced in it, and the measurement of the generated current yield allows for studying the performance of such samples. The light and energetic ion beam with a low flux, is used in the analysis by the ion beam induced charge (IBIC) method (Vittone et al., 2016; Lehn-

\*Corresponding author: [okakuee@aeoi.org.ir](mailto:okakuee@aeoi.org.ir)

<https://doi.org/10.22034/rpe.2024.437355.1181>

<https://dorl.net/dor/>

ert et al., 2017). Most of the required high-energy beams for the mentioned cases are not available in small-scale laboratories equipped with electrostatic accelerators since with the increase of beam energy, drastically not only the size and price of these accelerators and ancillary systems significantly increase, but also the radiation safety policy reduces the access to these accelerators. On the other hand, in the ion beam analysis methods, using nuclear reactions with high Q-value to analyze light elements in the sample is a well-known issue (Wang and Nastasi, 2010). In fact, light element measurements in the sample can be enhanced by nuclear reaction products with energies higher than the Rutherford scattering edge, which have a lower limit of detection.

In nuclear physics, the use of reaction products as a secondary beam has a long history. The radioactive ion beam, which plays a prominent role in the recognition of nuclei far from the stability line, is generated through nuclear spallation or nuclear reaction. In one method, the fragments resulting from the interaction of high-energy heavy ions with the target are produced with the help of a separator. In another method, the reaction products resulting from the collision of the high-energy ion from the accelerator with the target lead to the production of radioactive nuclei; by directing these radioactive nuclei and re-accelerating them, a radioactive ion beam is obtained. The ongoing development of the Radioactive Ion Beam (RIB) facility has extended the nuclides chart towards proton-rich, neutron-rich nuclei, and the drop lines towards heavier elements. After the initial utilization of radioactive beams at Bevalac, numerous facilities have been created to provide radioactive nuclear beams with an energy range of MeV to GeV. The RIB facilities at GANIL (France), GSI and FAIR (Germany), MSU (USA) and RIKEN (Japan) provide a wide range of radioactive beams and various measurements (Tanihata, 1995).

In addition to the technological advances of secondary ion beam extraction with specific mass and energy in major accelerator facilities, however, secondary ions have a vital rule in small-scale accelerator laboratories. For example, secondary ions can be used in MeV-SIMS (Janssens and Van Grieken, 2004). Moreover, to improve the sensitivity of ion beam analysis, experimental methods based on secondary probe such as PIXRF and K-edge contrast imaging of elements can be used (Farajipour Ghahroudi et al., 2019; Lamehi-Rachti et al., 2001). With the production of high-energy ion beam resulting from the interaction of neutrons with matter, access to high-energy ion projectiles has been reported (Mukhammedov et al., 2006, 2012).

In nuclear reactions documents, the ion collisions based on momentum conservation is classified into normal and inverse kinematics in which the incident beam is lighter or heavier than the target atom respectively. In nuclear physics, hydrogen and helium beams are considered as light ions and other ion beams are usually considered as heavy ions. In the center of mass frame (Fig. 1), when heavy projectiles collide with the light target materials, the heavy recoiled nuclei scatter at a smaller angle (compared to a light projectile to a heavy target) and simplify

the collection and purification (Yamaguchi et al., 2020).

These secondary ions have similar (but slightly lower) energy to the primary beam, so no re-acceleration is required. The energy of the secondary beam is adjusted by selecting the primary beam energy and target thickness (Yamaguchi et al., 2020). Indeed, the energy of the primary ion beam can be adjusted using the accelerator terminal voltage. Furthermore, as the ion beam traverses the target, it loses energy. Energy in the center of mass frame is defined as follows (Was et al., 2007):

$$E_{c.m} = \left( \frac{m_2}{m_1 + m_2} \right) E_{lab} \quad (1)$$

$$E_{c.m} + E_{frame} = E_{lab} \quad (2)$$

where  $E_{c.m}$  is the energy in the center of mass frame,  $E_{lab}$  is the energy in the laboratory frame,  $E_{frame}$  is the energy of the center of mass relative to laboratory frame and  $m_1$  and  $m_2$  are the masses of incident and target particles, respectively.

Secondary ions can be used as incident beam in other reactions. These secondary ions can have energy multiple times higher than the primary energy, while their flux will be much lower and will be a useful tool in cases where low flux ion is required due to the test conditions.

Due to the low intensity of current needed for studying semiconductor materials, there has been a search for suitable conditions to conduct research in this field. This particular study proposes the use of interactions resulting from light projectiles in a small electrostatic accelerator to generate high-energy secondary ions with low flux.

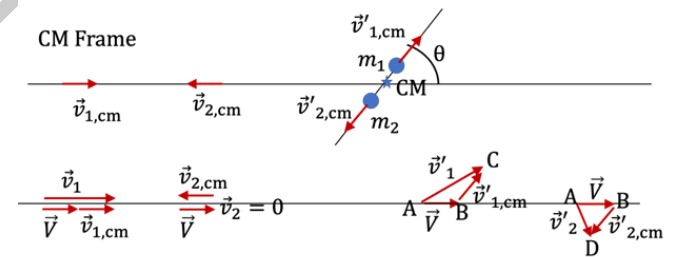


**Figure 1:** Typical representation of the collision in the center of mass frame.

## 2 Materials and Methods

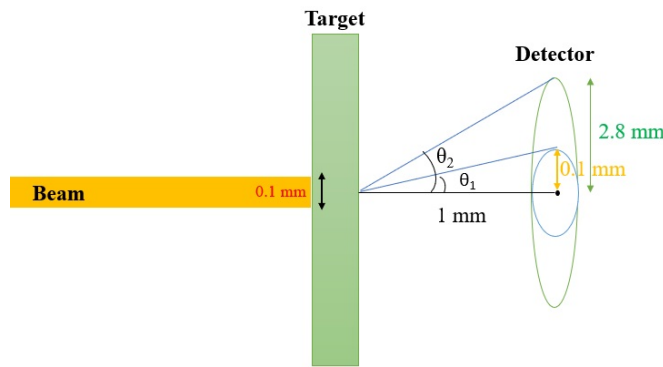
In this research, a KN3000 ion accelerator of VDG lab of the Nuclear Science and Technology Research Institute has been used. In this accelerator, proton, deuteron and helium beams up to 3 MeV energy are available. Due to issues related to radiation safety, the maximum deuteron energy is limited. In addition, like other laboratories, access to He-3 gas is limited due to its high price. The experimental setup was obtained based on 100 keV energy loss, with the sample thickness in the order of  $10^{19}$  atom.cm<sup>-2</sup>, the current  $\mu$ A ( $\sim 6 \times 10^{12}$  particles) and the solid angle 4.13 sr. Figure 2 is a general overview of the

**Table 1:** Selected nuclear reactions resulting from light particles of protons, deuterons and helium (<https://www.nndc.bnl.gov/qcalc/>). The reaction yields reported in the last column of the table are associated with  $70^\circ$ .

	Nuclear Reaction	$Q$ (MeV)	$E_{in}$ (MeV)	$E_{out}$ (MeV) ( $\theta_{lab} : 70, 50, 20$ )	Yield
1	${}^7\text{Li}(p,\alpha){}^4\text{He}$	17.35	1.5	10.065, 10.627, 11.183	$1.27 \times 10^6$
2	${}^{11}\text{B}(p,\alpha){}^8\text{Be}$	8.58	1.5	7.038, 7.354, 7.667	$0.14 \times 10^6$
3	${}^{15}\text{N}(p,\alpha){}^{12}\text{C}$	4.965	1.2	5.132, 4.962, 4.786	$0.05 \times 10^6$
4	${}^{19}\text{F}(p,\alpha){}^{16}\text{O}$	8.11	2.8	8.98, 9.275, 9.567	$0.58 \times 10^6$
5	${}^{14}\text{N}(d,p){}^{15}\text{N}$	8.61	1.7	9.722, 9.936, 10.146	$0.19 \times 10^6$
6	${}^{14}\text{N}(d,\alpha){}^{12}\text{C}$	13.58	1.7	11.884, 12.35, 12.81	$1.14 \times 10^6$
7	$\text{D}({}^3\text{He},\alpha)\text{P}$	18.35	1.5	5.64, 6.634, 7.16	$9.52 \times 10^6$
8	${}^{16}\text{O}({}^3\text{He},\alpha){}^{15}\text{O}$	4.9	2.42	5.995, 6.393, 6.785	$0.26 \times 10^6$
9	$\text{D}({}^3\text{He},p){}^4\text{He}$	18.35	1.5	16.47, 17.46, 18.455	$7.59 \times 10^6$

desired layout to obtain yield in this research. The vertical distance between the target and the charged-particle detector is 1 mm, the diameter of the beam is 0.2 mm, and the detector diameter including 0.2 mm hole diameter of the detector is 5.6 mm. With considered geometry, the angle  $\theta$  is approximately obtained  $70^\circ$ .

A thin target composed of pure Li was prepared for this study. Initially, a thin substrate of Au with a thickness of 510 nm was prepared using physical vapor deposition (PVD) technique and maintained in a self-supporting manner. Subsequently, a thin layer of Li with a thickness of 430 nm was deposited onto this self-support substrate using PVD technique. Due to the rapid absorption of environmental moisture by the Li layer, the prepared sample was immediately transferred to the reaction chamber.

**Figure 2:** General overview of arrangement and considered distances.

### 3 Results and Discussion

Considering the energy limit up to 3 MeV of the KN3000 accelerator available in the VDG Laboratory in Tehran and in order to expand the capability to access higher energetic ion beam for using in researches on the ion interaction with matter and materials analysis, this research performed by proton, deuteron and helium-3 projectile to access the secondary ions.

Then, among the nuclear reactions with significant  $Q$ -value, nuclear reactions are chosen in such a way that, while creating a suitable reaction yield, they do not lead to neutron production in the laboratory (or in some cases

with a very low probability) and comply with radiation protection requirements. Experimental setup of interaction was chosen in such a way that the yield of interaction is significant. The energy of the interaction products was calculated at different angles.

The yield of a reaction determines the number of interaction product atoms (Mukhammedov et al., 2008). To obtain yield ( $A$ ), Eq. (3) can be used, where  $N_i$  is the number of incident particles,  $\Omega$  is the solid angle,  $N_t$  is the number of target atoms per unit area,  $\sigma(E_a)$  is the cross-section, and  $\theta$  is the incident angle (Nastasi et al., 2014):

$$A = \frac{N_i \Omega \sigma(E_a) N_t}{\cos \theta} \quad (3)$$

The  $p+{}^{\text{nat}}\text{Li}$  measured spectra fitted using SIMNRA (Mayer, 1997) are shown in Fig. 3. The 1700 keV proton beam collides with a 400 nm thick  ${}^{\text{nat}}\text{Li}$  target on a 500 nm thick Au substrate perpendicularly, at the scattering angle of  $165^\circ$ . The products of this interaction have been measured using a  $300 \mu\text{m}$  silicon surface barrier detector. The two interaction products of  ${}^6\text{Li}(p,\alpha){}^3\text{He}$  and  ${}^7\text{Li}(p,\alpha)\alpha$  are indicated in the spectrum.

The high-energy alpha peak at 8 to 9 MeV is an evidence of a high-energy ion with low-yield that can be exploited to development of low-energy ion accelerator applications. A number of selected interactions are shown in Table 1.

In this table, the  $Q$ -value of reactions, the energy of reaction products at three angles of  $20^\circ$ ,  $50^\circ$  and  $70^\circ$ , as well as the reaction yield were obtained for the target thickness in the order of  $10^{19} \text{ atom.cm}^{-2}$  in  $1 \mu\text{A}$  beam-current and solid angle 4.13 sr. The obtained yields are related to the experimental cross sections with the closest angle to  $70^\circ$ . According to the number of incident particles which are in order of  $10^{12}$ , the number of secondary particles (flux) obtained is in order of  $10^9$ . The reaction yields reported in the last column of the table are associated with  $70^\circ$ .

Among the introduced reactions to access the high-energy proton and alpha beams, the reactions  $\text{D}({}^3\text{He},p){}^4\text{He}$ ,  $\text{D}({}^3\text{He},\alpha)\text{p}$ ,  ${}^{14}\text{N}(d,p){}^{15}\text{N}$  and  ${}^7\text{Li}(p,\alpha){}^4\text{He}$  have appropriate yield.

Access to light energetic particles with acceptable yields can lead to the development of using electrostatic ion accelerators for ion beam applications such as IBIC analysis and high energy ion implantation. One of the

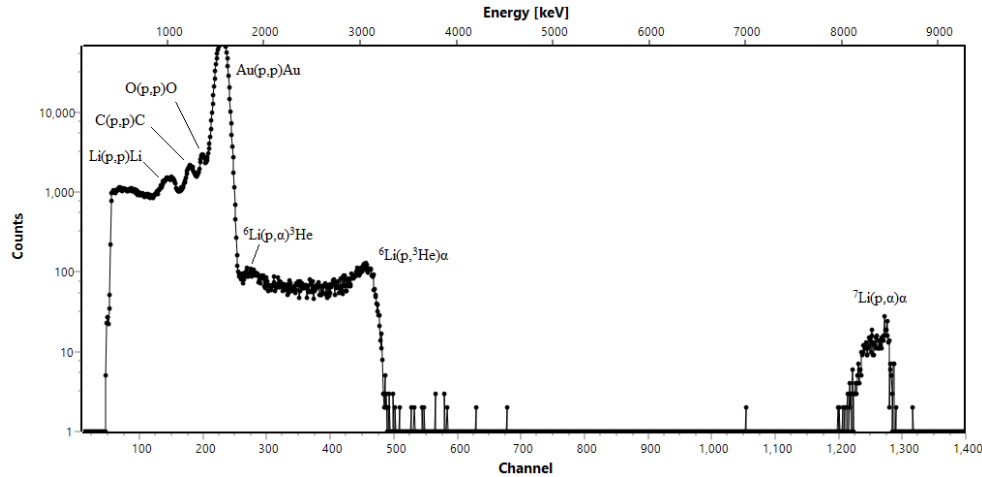


**Figure 3:** p+Li interaction products resulting from  $E_p = 1700$  keV beam on Li/Au target at  $\theta_{lab} = 120$ .

most important features of this method is not needing expensive accelerators for energetic ion beam applications with low flux. Although, the low flux resulting in these reactions fulfills need of high-energy beams with low flux, it may also present a limitation for utilizing these particles in high flux applications.

When the projectile collides to target in a nuclear reaction, reaction products of different atomic number, mass, and energy will be produced. With the help of stopping foil or magnetic/electrical analyzers, each of the reaction products can be separated (Salimi et al., 2021; Maslov et al., 2016). However, some points should be taken into account for production of high-quality secondary beam. The apparent thickness of target can cause the energy of the secondary particle to be dependent on the angle. In addition, the heterogeneity of the target is effective in the uniformity of the flux and energy of the secondary beam (Chu, 2012). To enhance production flux, employing an electromagnetic lens is a suitable approach.

Although the use of nuclear reaction products can easily expand the ion beam application, few research has been done in this field so far. The achievements of this research contribute to the development of ion beam applications. In this research, it has been shown that by nuclear reactions induced from a low-energy electrostatic accelerator and considering radiation safety protocols and without creating bulky physical shields, it is possible to access to energetic proton and alpha ion beams with low flux for research applications. The design of the laboratory arrangement is such that it can be easily implemented in the ion beam laboratory.

## 4 Conclusions

In this research, a proper source setup of light energetic ion beams with low flux in irradiating materials, biological samples and semiconductors was developed and designed for the laboratory equipped with low-energy electrostatic ion accelerators. For this purpose, the products of exothermic nuclear reactions have been used, which provide access to the required beam with low cost and

simpler equipment while considering radiation safety protocols. Favorable nuclear reactions for proton and alpha production with energy higher than 3 MeV were selected and their reaction yields were determined. Reactions with significant yield and high secondary particle energy were proposed for ion beam applications. By using the forward geometry, a proper setup was obtained for the production of the secondary beam. Reducing the distance between the secondary beam source and the target, the optimal yield is provided without the need for electromagnetic lenses.

## Acknowledgment

We are very grateful to the honorable director of the VDG lab of Nuclear Science and Technology Research Institute for their cooperation in providing the conditions and facilities to conduct this research.

## Conflict of Interest

The authors declare no potential conflict of interest regarding the publication of this work.

## References

- Bhandari, R. and Dey, M. K. (2011). Applications of accelerator technology and its relevance to nuclear technology. *Energy Procedia*, 7:577–588.
- Chu, W.-K. (2012). *Backscattering spectrometry*. Elsevier.
- Durante, M., Golubev, A., Park, W.-Y., et al. (2019). Applied nuclear physics at the new high-energy particle accelerator facilities. *Physics Reports*, 800:1–37.
- Farajipour Ghahroudi, N., Kakuee, O., and Yadollahzadeh, B. (2019). Imaging by the Use of Monochromatic X-Rays Induced by Proton Beam. *Journal of Nuclear Science and Technology (JONSAT)*, 39(4):1–10.

- Granja, C., Oancea, C., Mackova, A., et al. (2022). Energy Sensitive Imaging of Focused and Scanning Ion Microbeams with  $\mu\text{m}$  Spatial and  $\mu\text{s}$  Time Resolution. In *EPJ Web of Conferences*, volume 261, page 01007. EDP Sciences.
- Jamieson, D. N., Splatt, F., Pakes, C. I., et al. (2002). Single ion implantation in the quantum computer construction project. In *Nano-and Microtechnology: Materials, Processes, Packaging, and Systems*, volume 4936, pages 9–16. SPIE.
- Janssens, K. and Van Grieken, R. (2004). *Non-destructive micro analysis of cultural heritage materials*. Elsevier.
- Lamehi-Rachti, M., Oliay, P., Rahighi, J., et al. (2001). Application of PIXRF in the analysis of archaeological glazed tiles. *Nuclear Instruments and Methods in Physics Research Section B: Beam Interactions with Materials and Atoms*, 184(3):430–436.
- Lehnert, J., Meijer, J., Ronning, C., et al. (2017). Ion Beam Induced Charge analysis of diamond diodes. *Nuclear Instruments and Methods in Physics Research Section B: Beam Interactions with Materials and Atoms*, 404:259–263.
- Maslov, V., Kazacha, V., Kolesov, I., et al. (2016). Study of exotic weakly bound nuclei using magnetic analyzer MAVR. In *Journal of Physics: Conference Series*, volume 724, page 012033. IOP Publishing.
- Mayer, M. (1997). SIMNRA user's guide.
- McCallum, J. C., Jamieson, D. N., Yang, C., et al. (2012). Single-ion implantation for the development of si-based MOS-FET devices with quantum functionalities. *Advances in Materials Science and Engineering*, 2012.
- Mukhammedov, S., Khaidarov, A., and Barsukova, E. (2008). Be-7 yield produced in secondary reactions in a nuclear reactor. *Atomic Energy*, 104(1):82–84.
- Mukhammedov, S., Khaydarov, A., and Akramov, F. (2012). Nuclear Reactions Induced by Secondary Protons Formed under the Influence of Fast Neutrons.
- Mukhammedov, S., Khaydarov, A., and Barsukova, E. (2006). Nuclear reactions excited by recoil protons on a nuclear reactor.
- Nastasi, M., Mayer, J. W., and Wang, Y. (2014). *Ion beam analysis: fundamentals and applications*. CRC Press.
- Salimi, M., Kakuee, O., Masoudi, F., et al. (2021). Determination and benchmarking of  $^{27}\text{Al}(d, \alpha)$  and  $^{27}\text{Al}(d, p)$  reaction cross sections for energies and angles relevant to NRA. *Scientific Reports*, 11(1):18036.
- Tanihata, I. (1995). Nuclear structure studies from reaction induced by radioactive nuclear beams. *Progress in Particle and Nuclear Physics*, 35:505–573.
- Vittone, E., Pastuovic, Z., Breese, M. B., et al. (2016). Charge collection efficiency degradation induced by MeV ions in semiconductor devices: Model and experiment. *Nuclear Instruments and Methods in Physics Research Section B: Beam Interactions with Materials and Atoms*, 372:128–142.
- Wang, Y. and Nastasi, M. (2010). *Handbook of modern ion beam materials analysis*. MRS, Materials Research Soc.
- Was, G. S. et al. (2007). *Fundamentals of radiation materials science: metals and alloys*, volume 510. Springer.
- Yamaguchi, H., Kahl, D., and Kubono, S. (2020). Crib: the low energy in-flight ri beam separator. *Nuclear Physics News*, 30(2):21–27.

©2024 by the journal.

RPE is licensed under a [Creative Commons Attribution-NonCommercial 4.0 International License](https://creativecommons.org/licenses/by-nc/4.0/) (CC BY-NC 4.0).



#### To cite this article:

Imani, Z. S., Kakuee, O., Taghipour Azar, Y., Sabouri Dodaran, A. A. (2024). Exploring the applications of low energy ion accelerators through exothermic nuclear reaction products. *Radiation Physics and Engineering*, In Press.

DOI: [10.22034/rpe.2024.437355.1181](https://doi.org/10.22034/rpe.2024.437355.1181)

To link to this article: <https://doi.org/10.22034/rpe.2024.437355.1181>